



Investigation of the Noise Performance in SAR

Ms. Anamika Sharma, Dr. R.P. Singh and Dr. Sanjeev Gupta

*Department of Electronics and Communication Engineering,
AISECT University, Bhopal (Madhya Pradesh), INDIA*

(Corresponding author: Anamika Sharma)

(Received 09 January, 2016 Accepted, 27 February, 2016)

(Published by Research Trend, Website: www.researchtrend.net)

ABSTRACT: With the improvement of synthetic aperture radar (SAR) technology, larger areas are being imaged and the resolution of the images has increased. Larger images have to be transmitted and stored. Due to the limited storage and/or downlink capacity on the airplane or satellite, the volume of the data must be reduced. This makes compression of SAR images with minimal loss of information important. Mean squared error (MSE) and peak signal-to-noise ratio (PSNR) are the commonly quoted performance measures for comparing the compression algorithms. However, these measures inherently assume that the distortion is image independent noise, which is not a valid assumption in image compression algorithms. We propose a way to measure the distortion caused by compression and decompression of an image, by decoupling the distortion into a linear effect and additive uncorrelated noise, which models the nonlinear distortion. Using this procedure, the linear frequency distortion can be noise, is a high frequency effect, we use a discrete Laplacian operator to emphasize higher frequencies in the image and use a measure correlation measure to quantify this distortion.

I. INTRODUCTION

Synthetic Aperture Radar (SAR) is an active remote sensing system which has applications in Agriculture, ecology, geology, oceanography, hydrology and in the military SAR systems. Increase their effective aperture by using the motion of a satellite or an airplane they are mounted on. The primary reason which gives SAR systems such diverse applications is that they have the ability to take images in all weather conditions. With the improvement of SAR technology, larger areas are being imaged and the resolution of the images has increased. This causes larger images to be transmitted and stored. Due to the limited storage and/or downlink capacity on the airplane or satellite the data rate must be reduced. This motivates the compression of SAR images. The high entropy of SAR images results in very low compression ratios when lossless compression techniques are used. To achieve higher compression ratios, lossy image compression techniques are used. SAR data is inherently complex-valued but it is frequently converted to real data for interpretation by human observers or machine algorithms. However, when precise measurement of topographic elevation is required (interferometric SAR), the phase information is very important.

Thus to preserve this information accurately, lossless or near lossless compression is required. SAR imaging techniques introduce speckle noise, which is a form of multiplicative noise. The presence of speckle noise and the fact that more useful information is contained in the higher frequency bands make SAR images quite different from optical images. Due to these differences, classical image compression techniques do not perform as well when applied to SAR images. Although many different compression techniques have been applied to SAR images, they have been compared using peak signal-to-noise ratio or mean squared error. However, these measures inherently assume that the distortion is image independent noise, which is not a valid assumption in image compression algorithms. In this work, we propose three new quality metrics, which aim to quantify the linear and nonlinear distortions independently. Remote sensing is the acquisition of information about physical properties and phenomena without making any physical contacts. The remote sensing is classified into passive and active remote sensing, and the passive sensors detect microwave, visible, and infrared signals emitted from earth surface. The aerial photography, optical satellite, and passive microwave satellite are included in a device for passive remote sensing.

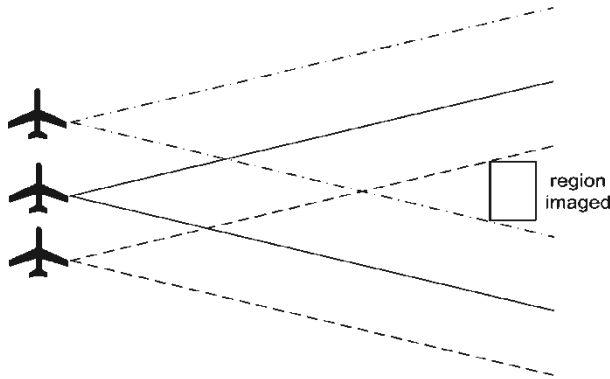


Fig. 1. Strip Map SAR Geometry.

Large virtual antenna (SAR). A SAR is advanced radar system that utilizes image processing techniques to synthesize a large virtual antenna, which provides much higher spatial resolution than is practical using a real-aperture radar (Curlander and McDonough, 1991). A SAR system transmits electromagnetic waves at a wavelength that can range from a few millimeter to tens of centimeters. Because a SAR system actively transmits and receives signals backscattered from the target area and the radar signals with long wavelengths are mostly unaffected by weather or clouds, a SAR can operate effectively during day and night and under most weather conditions. A chirp signal, in which the frequency is linearly modulated, is used for SAR processing, because a large bandwidth in range-time domain highly improves a range resolution and signal-to-noise ratio (SNR). Transmitted chirp signal ($s(t)$) has the form of Equation

$$s(t) = \text{rect}(tT) \times \exp\{2p f_0 t + p kt^2\}$$

II. RADAR CLASSIFICATIONS

Classification based on the primary function of radar is shown in the following figure

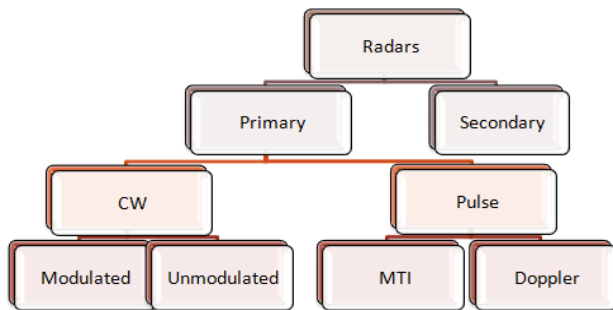


Fig. 2. Primary Radar Classifications.

Primary Radar. A Primary Radar transmits high-frequency signals toward the targets. The transmitted pulses are reflected by the target and then received by the same radar.

The reflected energy or the echoes are further processed to extract target information.

Secondary Radar. Secondary radar units work with active answer signals. In addition to primary radar, this type of radar uses a transponder on the airborne target object. A simple block diagram of secondary radar is shown below

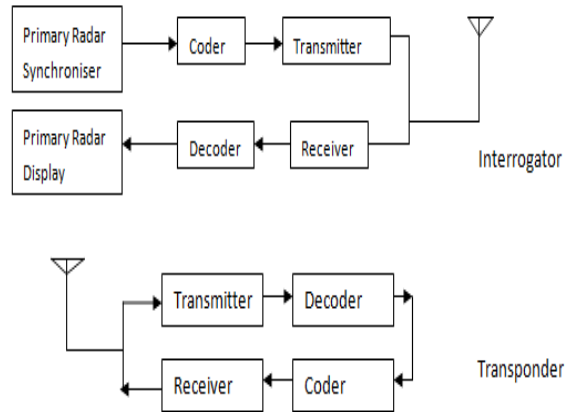


Fig. 3. Secondary Radar Classifications.

The ground unit, called interrogator, transmits coded pulses (after modulation) towards the target. The transponder on the airborne object receives the pulse, decodes it, induces the coder to prepare the suitable answer, and then transmits the interrogated information back to the ground unit. The interrogator/ground unit demodulates. The information is displayed on the display of the primary radar.

The secondary radar unit transmits and also receives high-frequency impulses, the so called interrogation. This isn't simply reflected, but received by the target by means of a transponder which receives and processes. After this the target answers at another frequency.

Various kinds of information like, the identity of aircraft, position of aircraft, etc. are interrogated using the secondary radar. The type of information required defines the MODE of the secondary radar.

Pulsed Radar. Pulsed radar transmits high power, high-frequency pulses toward the target. Then it waits for the echo of the transmitted signal for sometime before it transmits a new pulse. Choice of pulse repetition frequency decides the range and resolution of the radar.

Target Range and bearings can be determined from the measured antenna position and time-of-arrival of the reflected signal.

Pulse radars can be used to measure target velocities. Two broad categories of pulsed radar employing Doppler shifts are

• **MTI (Moving Target Indicator) Radar**

The MTI radar uses low pulse repetition frequency (PRF) to avoid range ambiguities, but these radars can have Doppler ambiguities.

• **Pulse Doppler Radar**

Contrary to MTI radar, pulse Doppler radar uses high PRF to avoid Doppler ambiguities, but it can have numerous range ambiguities.

Doppler Radars make it possible to distinguish moving target in the presence of echoes from the stationary objects. These radars compare the received echoes with those received in previous sweep. The echoes from stationary objects will have same phase and hence will be cancelled, while moving targets will have some phase change.

If the Doppler shifted echo coincides with any of the frequency components in the frequency domain of the received signal, the radar will not be able to measure target velocity. Such velocities are called blind speeds.

$$\text{Blind Speed} = n * \frac{c * PRF}{2 * f_0}$$

Where, f_0 = radar operating frequency.

Continuous Wave Radar:

CW radars continuously transmit a high-frequency signal and the reflected energy is also received and processed continuously. These radars have to ensure that the transmitted energy doesn't leak into the receiver (feedback connection). CW radars may be bistatic or monostatic; measures radial velocity of the target using Doppler Effect.

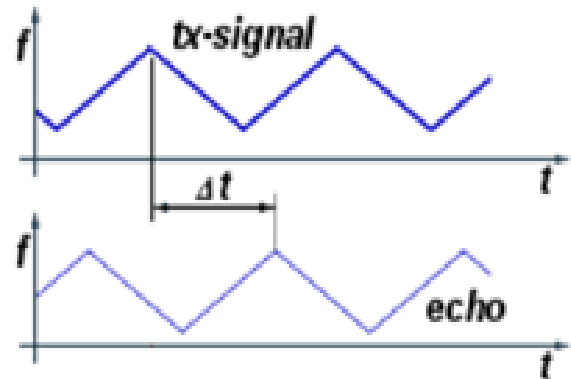
CW radars are of two types

1. Unmodulated. An example of unmodulated CW radar is speed gauges used by the police. The transmitted signal of these equipments is constant in amplitude and frequency. CW radar transmitting unmodulated power can measure the speed only by using the Doppler-effect. It cannot measure a range and it cannot differ between two reflecting objects.

2. Modulated. Unmodulated CW radars have the disadvantage that they cannot measure range, because run time measurements is not possible (and necessary) in unmodulated CW-radars. This is achieved in modulated CW radars using the frequency shifting method. In this method, a signal that constantly changes in frequency around a fixed reference is used to detect stationary objects. Frequency is swept repeatedly between f_1 and f_2 . On examining the received reflected frequencies (and with the knowledge of the transmitted frequency), range calculation can be done.

$$R = c * \Delta t / 2$$

where, R = range, Δt = time difference.



Ranging with a FMCW system

Fig. 4. Modulated Wave moving target.

If the target is moving, there is additional Doppler frequency shift which can be used to find if target is approaching or receding.

Frequency-Modulated Continuous Wave radars (FMCWs) are used in Radar Altimeters.

Operation of Basic Radar Systems

Radar is an acronym for Radio Detection and Ranging. The term "radio" refers to the use of electromagnetic waves with wavelengths in the so-called radio wave portion of the spectrum, which covers a wide range from 10^4 km to 1 cm. Radar systems typically use wavelengths on the order of 10 cm, corresponding to frequencies of about 3 GHz. The detection and ranging part of the acronym is accomplished by timing the delay between transmission of a pulse of radio energy and its subsequent return. If the time delay is Dt , then the range may be determined by the simple formula: $R = cDt/2$ where $c = 3 \times 10^8$ m/s, the speed of light at which all electromagnetic waves propagate. The factor of two in the formula comes from the observation that the radar pulse must travel to the target and back before detection, or twice the range. A radar pulse train is a type of amplitude modulation of the radar frequency carrier wave, similar to how carrier waves are modulated in communication systems. In this case, the information signal is quite simple: a single pulse repeated at regular intervals.

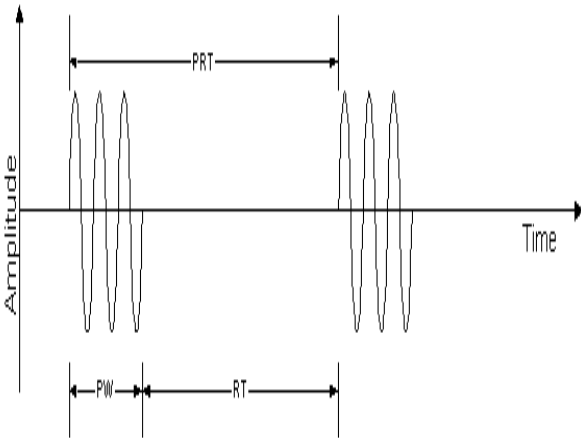


Fig. 5. Common radar carrier modulation wave.

The common radar carrier modulation, known as the pulse train is shown below. The common parameters of radar as defined by referring to Fig. 5. PW = pulse

width. PW has units of time and is commonly expressed in ms. PW is the duration of the pulse. RT = rest time. RT is the interval between pulses. It is measured in ms. PRT = pulse repetition time. PRT has units of time and is commonly expressed in ms. PRT is the interval between the start of one pulse and the start of another. PRT is also equal to the sum, PRT = PW+RT. PRF = pulse repetition frequency. PRF has units of time^{-1} and is commonly expressed in Hz ($1 \text{ Hz} = 1/\text{s}$) or as pulses per second (pps). PRF is the number of pulses transmitted per second and is equal to the inverse of PRT. RF = radio frequency. RF has units of time^{-1} or Hz and is commonly expressed in GHz or MHz. RF is the frequency of the carrier wave which is being modulated to form the pulse train.

Mechanization. A practical radar system requires seven basic components as illustrated below:

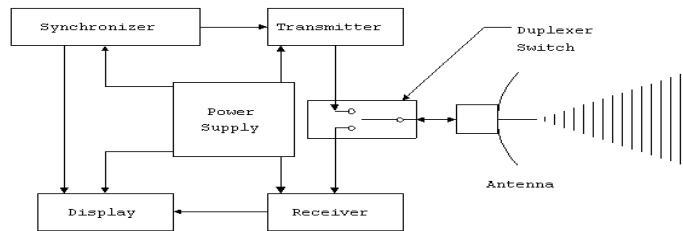


Fig. 6. Radar system basic block.

Transmitter. The transmitter creates the radio wave to be sent and modulates it to form the pulse train. The transmitter must also amplify the signal to a high power level to provide adequate range. The source of the carrier wave could be a Klystron, Traveling Wave Tube (TWT) or Magnetron. Each has its own characteristics and limitations.

Receiver. The receiver is sensitive to the range of frequencies being transmitted and provides amplification of the returned signal. In order to provide the greatest range, the receiver must be very sensitive without introducing excessive noise. The ability to discern a received signal from background noise depends on the signal-to-noise ratio (S/N).

The background noise is specified by an average value, called the noise-equivalent-power (NEP). This directly equates the noise to a detected power level so that it may be compared to the return. Using these definitions, the criterion for successful detection of a target is $P_r > (S/N) \text{ NEP}$, where P_r is the power of the return signal. Since this is a significant quantity in determining radar system performance, it is given a unique designation, S_{\min} , and is called the *Minimum Signal for Detection*.

$$S_{\min} = (S/N) \text{ NEP}$$

Since S_{\min} , expressed in Watts, is usually a small number, it has proven useful to define the decibel equivalent, MDS, which stands for *Minimum Discernible Signal*.

$$\text{MDS} = 10 \text{ Log} (S_{\min}/1 \text{ mW})$$

When using decibels, the quantity inside the brackets of the logarithm must be a number without units. In the definition of MDS, this number is the fraction $S_{\min} / 1 \text{ mW}$. As a reminder, we use the special notation dBm for the units of MDS, where the "m" stands for 1 mW. This is shorthand for decibels referenced to 1 mW, which is sometimes written as dB//1mW.

In the receiver, S/N sets a threshold for detection which determines what will be displayed and what will not. In theory, if $S/N = 1$, then only returns with power equal to or greater than the background noise will be displayed.

However, the noise is a statistical process and varies randomly. The NEP is just the average value of the noise. There will be times when the noise exceeds the threshold that is set by the receiver. Since this will be displayed and appear to be a legitimate target, it is called a *false alarm*.

If the SNR is set too high, then there will be few false alarms, but some actual targets may not be displayed known as a miss). If SNR is set too low, then there will be many false alarms, or a high false alarm rate (FAR).

Some receivers monitor the background and constantly adjust the SNR to maintain a constant false alarm rate, and therefore all called CFAR receivers. Some common receiver features are

1.) *Pulse Integration*. The receiver takes an average return strength over many pulses. Random events like noise will not occur in every pulse and therefore, when averaged, will have a reduced effect as compared to actual targets that will be in every pulse.

2.) *Sensitivity Time Control (STC)*. This feature reduces the impact of returns from sea state. It reduces the minimum SNR of the receiver for a short duration immediately after each pulse is transmitted. The effect of adjusting the STC is to reduce the clutter on the display in the region directly around the transmitter. The greater the value of STC, the greater the range from the transmitter in which clutter will be removed. However, an excessive STC will blank out potential returns close to the transmitter.

3.) *Fast Time Constant (FTC)*. This feature is designed to reduce the effect of long duration returns that come from rain. This processing requires that strength of the return signal must change quickly over its duration. Since rain occurs over an extended area, it will produce a long, steady return. The FTC processing will filter these returns out of the display. Only pulses that rise and fall quickly will be displayed. In technical terms, FTC is a differentiator, meaning it determines the rate of change in the signal, which it then uses to discriminate pulses which are not changing rapidly.

Power Supply. The power supply provides the electrical power for all the components. The largest consumer of power is the transmitter which may require several kW of average power. The actual power transmitted in the pulse may be much greater than 1 kW. The power supply only needs to be able to provide the average amount of power consumed, not the high power level during the actual pulse transmission. Energy can be stored, in a capacitor bank for instance, during the rest time. The stored energy then can be put into the pulse when transmitted, increasing the peak power. The peak power and the average power are related by the quantity called duty cycle, DC. Duty cycle is the fraction of each transmission cycle that the radar is actually transmitting. Referring to the pulse train in Figure 2, the duty cycle can be seen to be:

$$DC = PW / PRF$$

Synchronizer. The synchronizer coordinates the timing for range determination. It regulates that rate at which pulses are sent (i.e. sets PRF) and resets the timing clock for range determination for each pulse. Signals from the synchronizer are sent simultaneously to the transmitter, which sends a new pulse, and to the display, which resets the return sweep.

Duplexer. This is a switch which alternately connects the transmitter or receiver to the antenna. Its purpose is to protect the receiver from the high power output of the transmitter. During the transmission of an outgoing pulse, the duplexer will be aligned to the transmitter for the duration of the pulse, PW. After the pulse has been sent, the duplexer will align the antenna to the receiver. When the next pulse is sent, the duplexer will shift back to the transmitter. A duplexer is not required if the transmitted power is low.

Antenna. The antenna takes the radar pulse from the transmitter and puts it into the air. Furthermore, the antenna must focus the energy into a well-defined beam which increases the power and permits a determination of the direction of the target. The antenna must keep track of its own orientation which can be accomplished by a synchro-transmitter. There are also antenna systems which do not physically move but are steered electronically (in these cases, the orientation of the radar beam is already known a priori).

The beam-width of an antenna is a measure of the angular extent of the most powerful portion of the radiated energy. For our purposes the main portion, called the main lobe, will be all angles from the perpendicular where the power is not less than 1/2 of the peak power, or, in decibels, -3 dB. The beam-width is the range of angles in the main lobe, so defined. Usually this is resolved into a plane of interest, such as the horizontal or vertical plane. The antenna will have a separate horizontal and vertical beam-width. For a radar antenna, the beam-width can be predicted from the dimension of the antenna in the plane of interest $q = \lambda/L$ where: q is the beam-width in radians, λ is the wavelength of the radar, and L is the dimension of the antenna, in the direction of interest (i.e. width or height). In the discussion of communications antennas, it was stated that the beam-width for an antenna could be found using $q = 2\lambda/L$. So it appears that radar antennas have one-half of the beam-width as communications antennas. The difference is that radar antennas are used both to transmit and receive the signal. The interference effects from each direction combine, which has the effect of reducing the beam-width. Therefore when describing two-way systems (like radar) it is appropriate to reduce the beam-width by a factor of 1/2 in the beam-width approximation formula.

The directional gain of an antenna is a measure of how well the beam is focused in all angles. If we were restricted to a single plane, the directional gain would merely be the ratio $2\pi/q$. Since the same power is distributed over a smaller range of angles, directional gain represents the amount by which the power in the beam is increased. In both angles, then directional gain would be given by: $G_{dir} = 4\pi/qf$ since there are 4π steradians corresponding to all directions (solid angle, measured in steradians, is defined to be the area of the beam front divided by the range squared, therefore a non-directional beam would cover an area of $4\pi R^2$ at distance R , therefore 4π steradians). Here we used:

q = horizontal beam-width (radians)
 f = vertical beam-width (radians)

Sometimes directional gain is measured in decibels, namely $10 \log(G_{dir})$. As an example, an antenna with a horizontal beam-width of 1.5° (0.025 radians) and vertical beam-width of 20° (0.33 radians) will have: directional gain(dB) = $10 \log(4\pi / 0.025 \cdot 0.333) = 30.9$ dB

Pulse Width. The duration of the pulse and the length of the target along the radial direction determine the duration of the returned pulse. In most cases the length of the return is usually very similar to the transmitted pulse. In the display unit, the pulse (in time) will be

converted into a pulse in distance. The range of values from the leading edge to the trailing edge will create some uncertainty in the range to the target. Taken at face value, the ability to accurately measure range is determined by the pulse width. If we designate the uncertainty in measured range as the range resolution, R_{RES} , then it must be equal to the range equivalent of the pulse width, namely: $R_{RES} = c \cdot PW/2$. Now, you may wonder why not just take the leading edge of the pulse as the range which can be determined with much finer accuracy? The problem is that it is virtually impossible to create the perfect leading edge. In practice, the ideal pulse will really appear like:

III. RESULTS

The proposed Investigation of the Noise Performance in SAR is simulated by using MATLAB 7.8.0. MATLAB is a strong mathematical tool which provides help to engineers to solve, model, simulate the problems and find solutions assuming environment in to mathematical equations. It is standard engineering tool as it perform many different tasks using different tool box relevant to different particular cases e.g. Control systems, signal processing, image processing, communication systems, and support complex matrix manipulation, simulink etc.

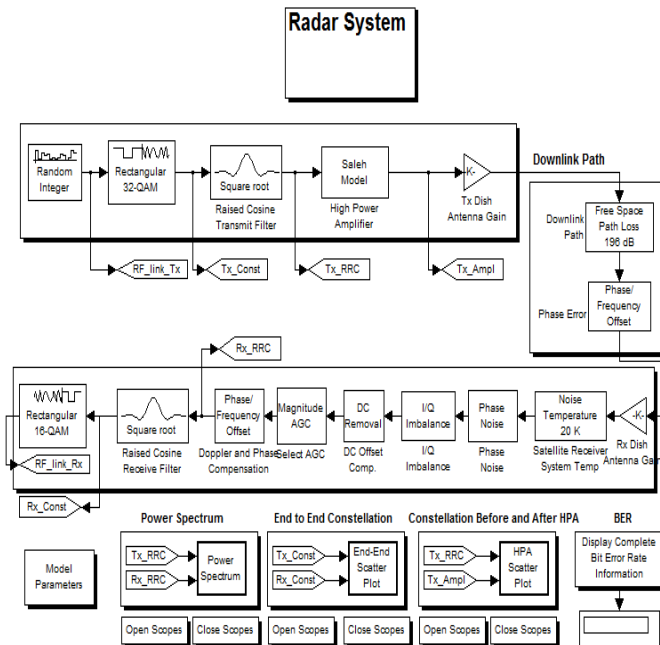


Fig. 7. SAR Simulation system.

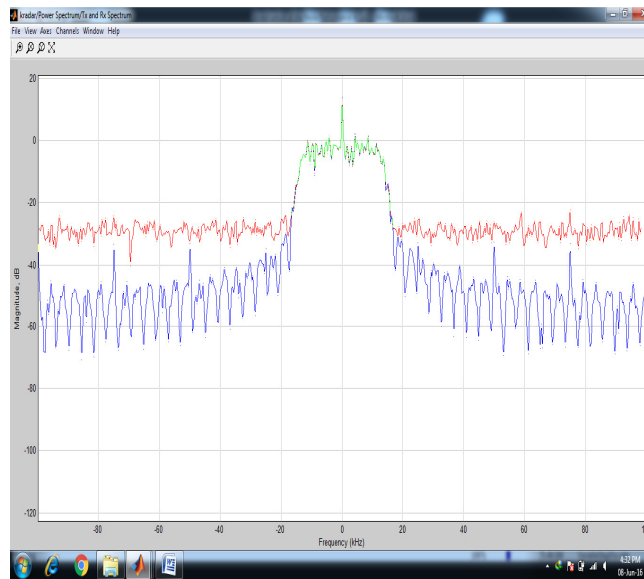


Fig. 8. SAR Simulation system.

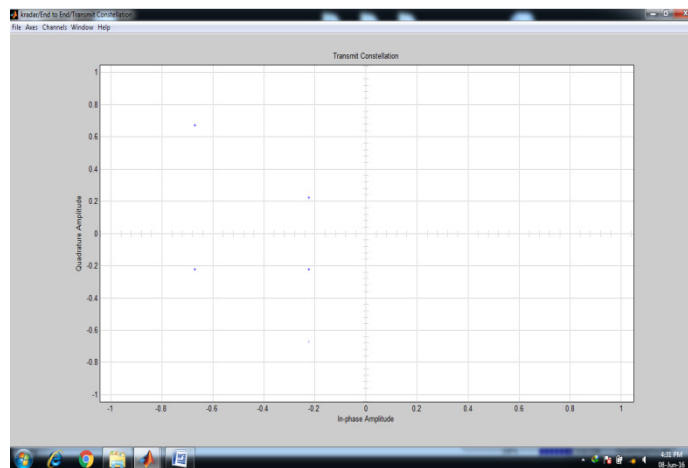


Fig. 9. SAR Simulation system.

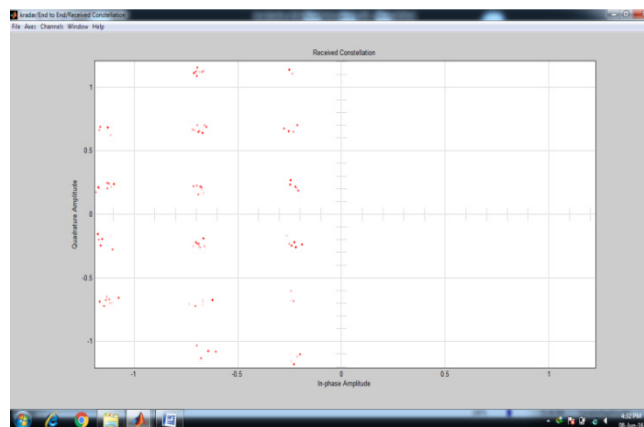


Fig. 10. SAR Simulation system.

In different research field it provides platform for learning and comparison of theoretical hypothesis and simulated values. It even provides support to nonlinear system calculations and result. In the simulation process, the goal was to reach.

CONCLUSIONS

Although they are commonly used, standard performance measures such as MSE and PSNR are not appropriate measures for SAR image compression algorithms. This follows from the fact that these metrics are noise measures and assume signal independent noise which is not a valid assumption in image compression algorithms. In this work we propose a new framework for evaluating the distortion introduced by compression. We measure the linear distortion by modeling the compression-decompression procedure as a linear filtering operation followed by the addition of uncorrelated noise. Both the linear distortion measure and the noise quality measure can be weighted in frequency domain depending on the application. We use the contrast sensitivity function, which is based on a linear model of the human visual system, to weight these measures assuming the decompressed images are consumed by humans. With high compression ratios, however, the additive noise approximation is invalid and the noise measures are inappropriate. In this case we use the correlation of edge information, which gives us a better measure of the nonlinear distortion, since the distortion is primarily a high frequency effect. We have tested the metrics on several SAR images and conclude that these metrics give more consistent results compared to the commonly applied metrics. A model for the distribution of the estimated look cross spectrum, which has the coherence as a key parameter. The model provides pdfs for the phase, magnitude as well as the real and imaginary part of the cross spectrum depending on the amount of smoothing applied in the estimation. The coherence was factored into two components with the first one describing ML phase estimation was demonstrated to be appropriate for In SAR processing of single pass high resolution multi baseline airborne data. Careful calibration steps were necessary to make the data fit the ML model assumptions. For example, an elevation angle dependent phase correction was applied for each slave channel.

ML method. These were found to be statistically significant, confirming the hypothesis stated in the introduction that ML method results in a lower phase noise than method. Outliers were discarded from the data to compute the phase standard deviation. They were mostly found when using low numbers of looks. These outliers will be further studied, including their distribution and their dependency on the Processing method, the local coherence, and the number of looks.

REFERENCES

- [1] H. Klausing, "Feasibility of a synthetic aperture radar with rotating antennas (ROSAR)," in *Proc. 19th Eur. Microw. Conf.*, London, U.K., 1989, pp. 287–299.
- [2] F. Ali, A. Urban, and M. Vossiek, "A high resolution 2-D omni-directional synthetic aperture radar scanner at band," in *Proc. 7th Eur. Radar Conf.*, Paris, France, 2010, pp. 503–506.
- [3] N. Marechal, "High frequency phase errors in SAR imagery and implications for autofocus," in *Proc. IEEE Int. Geosci. Remote Sens. Symp.*, Lincoln, NE, USA, 1996, vol. 2, pp. 1233–1240.
- [4] D. E. Wahl, P. H. Eichel, D. C. Ghiglia, and C. V. Jakowatz, "Phase gradient autofocus a robust tool for high resolution SAR phase correction," *IEEE Trans. Aerosp. Electron. Syst.*, vol. 30, no. 3, pp. 827–835, Jul. 1994.
- [5] S. Wang and X. Huang, "Autofocus techniques for reducing phase errors in UWB-SAR," in *Proc. IEEE Nat. Aerosp. Electron. Conf.*, Dayton, OH, USA, 1997, pp. 1009–1010.
- [6] R. P. Perry, R. C. Dipietro, and R. L. Fante, "SAR imaging of moving targets," *IEEE Trans. Aerosp. Electron. Syst.*, vol. 35, no. 1, pp. 188–200, Jan. 1999.
- [7] R. P. Perry, R. C. Di Pietro, B. Johnson, A. Kozma, and J. J. Vaccaro, "Planar subarray processing for SAR imaging," in *Rec. IEEE Int. Radar Conf.*, Alexandria, VA, USA, 1995, pp. 473–478.
- [8] S. Nordebo, Z. Zang, and I. Claesson, "A semi-infinite quadratic programming algorithm with applications to array pattern synthesis," *IEEE Trans. Circuits Syst. II, Analog Digit. Signal Process.*, vol. 48, no. 3, pp. 225–232, Mar. 2001.
- [9] C. Ozdemir, *Inverse Synthetic Aperture Radar Imaging With MATLAB Algorithms.* New York, NY, USA: Wiley, 2012, pp. 299–342.
- [10] J. C. Kirk, "Motion compensation for synthetic aperture radar," *IEEE Trans. Aerosp. Electron. Syst.*, vol. AES-11, no. 3, pp. 338–348, May 1975.
- [11] M. Xing, X. Jiang, R. Wu, F. Zhou, and Z. Bao, "Motion compensation for UAV SAR based on raw radar data," *IEEE Trans. Geosci. Remote Sens.*, vol. 47, no. 8, pp. 2870–2883, Aug. 2009.

- [12]. D. A. Ausherman, A. Kozma, J. L. Waker, H. M. Jones, and E. C. Poggio, "Developments in radar imaging," *IEEE Trans. Aerosp. Electron. Syst.*, vol. **AES-20**, no. 4, pp. 363–400, Jul. 1984.
- [13]. V. C. Chen and S. Qian, "Joint time-frequency transform for radar range-Doppler imaging," *IEEE Trans. Aerosp. Electron. Syst.*, vol. **34**, no. 2, pp. 486–499, Apr. 1998.
- [14]. A. Moreira and Y. Huang, "Airborne SAR processing of highly squinted data using a chirp scaling approach with integrated motion compensation," *IEEE Trans. Geosci. Remote Sens.*, vol. **32**, no. 5, pp. 1029–1040, Sep. 1994.
- [15]. H. Ermert and J. O. Schaefer, "Flaw detection and imaging by high resolution synthetic pulse holography," in *Proc. 10th Int. Acoust. Imag. Symp.*, 1980, pp. 629–642.
- [16]. M. Vossiek, A. Urban, S. Max, and P. Gulden, "Inverse synthetic aperture secondary radar concept for precise wireless positioning," *IEEE Trans. Theory Techn.*, vol. **55**, no. 12, pp. 2447–2453, Dec. 2007.
- [17]. F. Ali, A. Urban, and M. Vossiek, "A short range synthetic aperture imaging radar with rotating antenna," *Int. J. Electron. Telecommun.*, vol. **57**, pp. 97–102, Mar. 2011.
- [18]. F. Ali and M. Vossiek, "Detection of weakmoving targets based on 2-D range-Doppler FMCW radar Fourier processing," in *Proc. 5th German Microw. Conf.*, Berlin, Germany, 2010, pp. 214–217.
- [19]. M. Vossiek, S. Max, and P. Gulden, "Imaging method utilizing a synthetic aperture, method for determining a relative velocity between a wave-based sensor and an object, or apparatus for carrying out the methods," U.S. Patent 0321235 A1, Dec. 23, 2010.
- [20]. M. Vossiek, P. Heide, M. Nalezinski, and V. Magori, "Novel FMCW radar system concept with adaptive compensation of phase errors," in *Proc. 26th Eur. Microw. Conf.*, Prague, Czech Republic, 1996, pp. 135–139.
- [21]. A. Nosich, R. Sauleau, and Y. V. Gandel, "Classical ADE and PACO omni-directional dual reflector antennas simulated in 2-D using a Nystrom-type MDS algorithm," in *Proc. 39th Eur. Microw. Conf.*, Rome, Italy, 2009, pp. 858–861.
- [22]. W. Menzel and R. Leberer, "Folded reflect array antennas for shaped beam applications," in *Proc. 1st Eur. Antennas Propag. Conf.*, Nice, France, 2006, pp. 1–4.
- [23]. J. Richter and L.-P. Schmidt, "Dielectric rod antennas as optimized feed elements for focal plane arrays," in *Proc. IEEE AP-S Int. Symp.*, Washington, DC, USA, 2005, vol. **3A**, pp. 667–670.
- [24]. J. Richter, M. Müller, and L.P. Schmidt, "Measurement of phase centers of rectangular dielectric rod antennas," in *Proc. IEEE AP-S Int. 1 Cumming, I.G., Wong, F.H.: 'Digital processing of synthetic aperture radar data: algorithms and implementation' (Artech House, Norwood, MA, 2005)*
- [25]. Chen, S.W., Sato, M.: 'Tsunami damage investigation of built-up areas using multi-temporal spaceborne full polarimetric SAR images', *IEEE Trans. Geosci. Remote Sens.*, 2013, **51**, (4), pp. 1985–1997
- [26]. Zhou, F., Zhao, B., Tao, M.L., et al.: 'A large scene deceptive jamming method for space-borne SAR', *IEEE Trans. Geosci. Remote Sens.*, 2013, **51**, (8), pp. 4486–4495
- [27]. Zhou, F., Xing, M.D., Bai, X.R., et al.: 'Narrowband interference suppression for SAR based on complex empirical mode decomposition', *IEEE Geosci. Remote Sens. Lett.*, 2009, **6**, (3), pp. 423–427
- [28]. Zhou, F., Xing, M.D., Bai, X.R., et al.: 'A novel method for adaptive SAR barrage jamming suppression', *IEEE Geosci. Remote Sens. Lett.*, 2012, **9**, (2), pp. 292–296
- [29]. Feng, J., Zheng, H.F., Deng, Y.K., et al.: 'Application of subband spectral cancellation for SAR narrow-band interference suppression', *IEEE Trans. Geosci. Remote Sens. Lett.*, 2012, **9**, (2), pp. 190–193
- [30]. Huang, L., Dong, C.X., Shen, Z.B., et al.: 'The influence of rebound jamming on SAR GMTI', *IEEE Trans. Geosci. Remote Sens. Lett.*, 2015, **12**, (2), pp. 399–403.